STUDIES AND RESEARCHES – V. 29, 2009
Graduate School in Concrete Structures – Fratelli Pesenti
Politecnico di Milano, Italy

MODELLING TECHNIQUES TO CAPTURE THE BACKBONE ENVELOPE BEHAVIOUR OF COUPLING BEAMS SUBJECTED TO SEISMIC LOADING

Sergio Breña[1], Miguel Fernández Ruiz[2], Neven Kostic[3] and Aurelio Muttoni[4]

ABSTRACT

Structural R/C cores are a popular and efficient choice as lateral-load resisting system in medium to tall buildings. The walls of the cores typically present large openings providing access to elevators placed within them. Shear induced by lateral forces has thus to be transmitted by limited portions of the core (wall between openings) which are commonly named coupling beams. Such beams are subjected to large deformation demands as the system undergoes lateral displacements associated to wind or earthquake forces, and typically govern the response of the structural system. Performance-based assessment and design of these members have been gaining popularity within the structural engineering community approximately during the last 15 years. These techniques rely on accurate definitions of component behavior (shear force – chord rotation) for their successful application to overall system performance. In current seismic design and assessment documents, the influence of some instrumental parameters such as slenderness, reinforcement layout or even failure mode is not (or only partly) addressed. In this paper, the influence of these parameters is investigated on the basis of the results of an experimental campaign. Several approaches to generate force-deformation envelope (backbone) curves for coupling beams are discussed and compared. The use of stress field models is introduced as a promising technique to rationally represent the backbone envelope behavior of elements subjected to cyclic loading.

[1]Associate Professor. University of Massachusetts Amherst, USA (on sabbatical leave at Ecole Polytechnique Fédérale de Lausanne during Spring 2009).
[2] Lecturer, Ecole Polytechnique Fédérale de Lausanne, Switzerland.
[3] Researcher, Ecole Polytechnique Fédérale de Lausanne, Switzerland.
[4] Professor, Ecole Polytechnique Fédérale de Lausanne, Switzerland.

1. INTRODUCTION

Most medium to tall buildings resist horizontal loading (earthquake or wind) through interior reinforced concrete cores (Figs. 1.1a,b). Such horizontal actions usually govern structural design of the cores, which in turn control the deformability of the building (Fig. 1.1c).

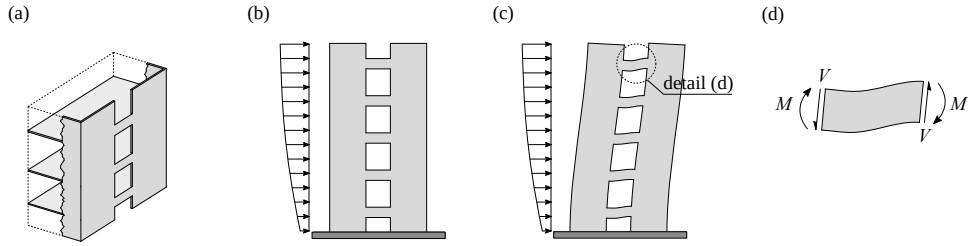

Figure 1.1 – Coupling beams in reinforced concrete cores: (a) view of a core with openings; (b) core subjected to horizontal loading; (c) deformation of the core; and (d) internal forces developing in a coupling beam

In order to provide access to elevators or other facilities, cores usually have aligned openings (Fig. 1.1a), implying that shear forces have to be carried by only limited portions of the cores (coupling beams between openings). Coupling beams are subjected to relatively large internal forces (bending and shear (Fig. 1.1d), causing them to be the controlling element in the overall response of the wall system (shear failure of coupling beams cause a loss in wall coupling effect).

1.1 Summary of existing research on coupling beams

Initial experimental research on reinforced concrete coupling beams concentrated on the development of reinforcing bar details to improve ductility under cyclic actions. Prior to the mid-1970s the most commonly used reinforcement pattern in coupling beams consisted of an orthogonal arrangement of longitudinal and transverse bars (conventional reinforcement, refer to fig. 1.2a). Failure of the Mt. McKinley apartment building during 1964 Alaska earthquake demonstrated that beams with a conventional reinforcement pattern and small amounts of transverse reinforcement could fail in a brittle manner under strong ground shaking and prompted researchers to develop alternative reinforcement configurations that would promote ductile behavior of coupling beams.

In the early 1970s, Paulay and several collaborators at the University of Canterbury, New Zealand, conducted monotonic and cyclic tests of coupling beams with different reinforcement patterns (Paulay 1971a, 1971b). Through their studies they identified the two predominant shear failure modes that occur in conventionally reinforced coupling beams: diagonal tension failures, and sliding shear failures. Their tests indicated that diagonal tension failures might occur at low-to-moderate ductility demands even if beams yield initially in flexure.

Additionally, for beams with low clear span-to-depth ratio and high amounts of transverse reinforcement designed to preclude diagonal tension failures, sliding shear failures occurred at higher deformation demands due to accumulation of plastic strain in the longitudinal reinforcement and damage accumulation of concrete near the beam ends. To promote ductility, Paulay proposed a reinforcement pattern consisting of sets of diagonally placed bars extending from corner to corner of coupling beams (Fig. 1.2b) following observed cracking patterns in laboratory tests and to avoid premature failures associated with low ductilities due to crack widening at beam ends (Paulay 1971b; Paulay and Binney 1974). To avoid buckling, diagonal bars are typically laterally supported using closely spaced hoops because they are expected to undergo large inelastic load reversals.

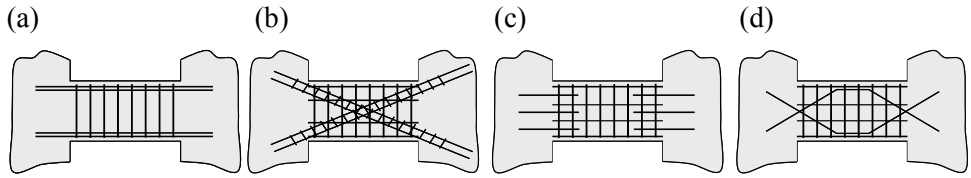

Figure 1.2 – Reinforcement patterns in coupling beams: (a) conventionally reinforced beams; (b) diagonally reinforced beams; (c) beams with dowel bars at ends; and (d) rhombic reinforcement pattern

Paulay and Santhakumar (1976) compared the effect of coupling beam reinforcement pattern on lateral-load response of coupled wall systems by testing one-quarter scale coupled wall models with conventionally reinforced beams or diagonally reinforced beams. Their results indicated that sliding shear failure could occur at the end of conventionally reinforced coupling beams after several cycles of shear reversal. In contrast, beams with diagonal reinforcing bars exhibited stable response without strength or stiffness degradation at large displacements. Current and past codes (*UBC 1997*; *IBC 2009*; *ACI 318-08*) promote use of diagonal bars in coupling beams with low aspect ratios and high shear stresses.

Diagonally reinforced beams, however, have proved difficult to build in practice due to reinforcement congestion, horizontal and vertical bar interference, and the need for confinement reinforcement. With the goal of simplifying construction without sacrificing ductile response, several investigators have proposed alternate reinforcement configurations that would improve the performance of coupling beams under large load reversals (Barney et al. 1980; Tassios, Moretti, and Bezas 1996; Galano and Vignoli 2000). Some of the configurations that have been proposed are shown in Figure 1.2c,d. Other investigators have developed hybrid coupling beams by using structural steel elements embedded within the reinforced concrete beam cross section (Harries et al. 1997). Recent studies have also suggested the use of high-performance fiber-reinforced cement composites with

high tensile strength to simplify detailing of coupling beams for new construction (Canbolat, Parra-Montesinos, and Wight 2005). All these techniques are extremely promising for new buildings, but little has been done on the systematic development of rehabilitation techniques of vulnerable coupling beams that may have older reinforcing details.

A large number of research studies concentrating on elastic analysis techniques were conducted in the 1960s to calculate parameters that affect the elastic response of coupled wall systems (e.g. Beck 1962; Coull and Choudhury 1967; Coull and Puri 1968; Coull, Puri, and Tottenham 1973). From these analytical studies, parameters that controlled the lateral strength of the system such as degree of coupling were established. It was later found that the earthquake response of coupled wall systems could not be accurately estimated using elastic analysis techniques, so research studies concentrated on development of nonlinear analysis methods for coupled wall structures (Paulay 1970; Glueck 1973; Elkholy and Robinson 1974; Takayanagi and Schnobrich 1979). Mahin and Bertero (1976) conducted nonlinear dynamic analyses of planar models representing the coupled core of the Banco de America Building, which was moderately damaged during the 1972 Managua earthquake. Three different force-deformation curves representing behavior of the coupling beams were studied to include the possibility of brittle shear failure or ductile flexural failure (with and without strength degradation) of coupling beams. Additionally two different ground motion records were used in the analyses. Analysis results indicated that the number of inelastic excursions of coupling beams might significantly exceed the number of cycles of roof displacement due to higher mode effects. It was found that elastic analyses did not provide realistic estimates of deformation or internal actions generated in coupled wall systems. These analytical studies have provided a strong foundation for current practice in the analysis of coupled wall structures. More importantly, these studies highlighted the importance of using nonlinear techniques to obtain better estimates of expected seismic response of coupled wall systems.

1.2 Static-nonlinear methods for seismic performance-based evaluation of coupling beams

Standard ASCE/SEI 41-06 – Seismic Rehabilitation for Existing Buildings (2006) has become a common resource for structural engineers involved in evaluation and rehabilitation of existing buildings since its publication. This standard evolved from *FEMA 356 – Prestandard and Commentary for the Seismic Rehabilitation of Buildings* (2000), a document which was used for several years in rehabilitation projects by engineers within the United States. These documents were developed in order to guide engineers in the performance-based rehabilitation process required for seismically vulnerable buildings.

One of the first steps in the performance-based rehabilitation process is to evaluate the force and displacement capacity of an existing structure. *ASCE/SEI*

41-06 provides details for various nonlinear analysis techniques that can be used by engineers in the evaluation process, including dynamic time-history or static (pushover) techniques. To date because of its ease of application and availability of commercial software to conduct the analysis, the static nonlinear analysis (pushover) technique has been used amply by structural engineers in the evaluation process. In this analysis technique the response of the structure is calculated by capturing the nonlinear response of individual components of the system using their respective force-deformation relationship. Individual component force-deformation relationships in combination with a model of the structural system are believed to provide an acceptable estimate to the overall structural response. It is assumed that nonlinear behavior is restricted to specific zones depending on the structural system, a simplification that is often acceptable. In the case of coupled-wall structures, these nonlinear zones are concentrated either within the coupling beams or near the base of the structural walls where bending moments due to lateral forces are greatest. The system is then subjected to a set of lateral forces with a prescribed pattern that is increased until a mechanism is formed. The calculated monotonic nonlinear force-displacement response of the structural system can be plotted and compared with acceptable lateral displacement (or drift) values for different levels of performance (e.g. immediate occupancy, life safety, collapse prevention).

In coupled wall systems, component force-deformation envelopes (backbones) are typically used instead of modeling the complete hysteretic behavior of coupling beams. Coupling beam force-deformation curves are constructed using shear force and chord rotation, respectively. The accuracy of the nonlinear static analysis will obviously depend on the quality of the backbone curve of an element and the techniques by which these are determined. It is believed that insufficient guidance is provided in *ASCE/SEI 41-06* to construct these backbone curves for coupling beams. Therefore, a critical review of the techniques contained in this document is presented here.

1.2.1 Calculation of coupling beam strength – ASCE/SEI 41-06

According to *ASCE/SEI 41-06*, to construct the shear force-chord rotation envelope of coupling beams the shear strength of coupling beams may be estimated using techniques in the *ACI Building Code* (*ACI 318-08*) employing actual (or expected) material strengths and a strength reduction factor (or partial safety factors) equal to 1.0 in all equations. The expected flexural strength is calculated accounting for multiple layers of longitudinal reinforcement if present in the beam. Bending moments can be related to beam shear force from equilibrium considerations by assuming an effective length of the beams. The shear force in the beams will then depend on the plastified length at the beam ends. For little yield spreading in the longitudinal reinforcement (such as for the

condition at yield or brittle shear failure modes), end moments may be assumed acting at the beam-wall connection, but for conditions where significant yield penetration has occurred (stable plastic hinging at anticipated flexural strength) moments are assumed to act at the end of the plastified region. Thus, shear forces corresponding to these two conditions can be calculated using Eqs. (1a) and (1b), respectively:

$$V_{end} = \frac{2M}{l_n} \qquad (1a) \qquad\qquad V_{hinge} = \frac{2M}{l_n - l_p} \qquad (1b)$$

where M corresponds to the moment at the end of the beams, l_n is the beam clear span, and l_p is an assumed plastic hinge length. The recommended plastic hinge length in *ASCE/SEI 41-06* is the beam flexural depth divided by 2. In short deep members such as coupling beams the shear force required to develop hinging may be quite large as the difference between the clear span and plastic hinge length can be very small (it approaches zero when $l_n = h$).

Coupling beam shear strength (diagonal tension) is calculated using (*ACI 318-08* Eq. 21-7), which for normalweight concrete is:

$$V_n = A_{cv}\left(\alpha_c \sqrt{f_c'} + \rho_v f_{yt}\right) \qquad (2)$$

where α_c is equal to 3 for a clear span to depth ratio $l_n/h < 1.5$, or 2 for $l_n/h > 2$ (linear interpolation is conducted for values in between); $\rho_v = A_v/(b_w s)$ is the transverse reinforcement ratio; A_{cv} is the cross sectional area of the beam parallel to the application of shear force; b_w is the beam web width; f_{yt} is the expected yield stress of transverse reinforcement at a spacing s. One of the limitations of Eq. 2 is that it does not recognize the shear strength degradation that occurs with beam cycling, nor other shear failure modes that can occur and that have been documented for coupling beams (e.g. sliding shear). This could be due to strength degradation or sliding shear modes typically occurring at higher deformation demands. Other available documents provide more detailed procedures to estimate shear strength as a function of displacement ductility (*FEMA 306*, for example).

1.2.2 Chord rotation as deformation parameter

The most widely used deformation parameter to construct backbone curves for coupling beams is chord rotation. Coupling beam chord rotations are estimated using the tabulated values (modeling parameters) listed in Table 1.1, which are reproduced from *ASCE/SEI 41-06*. These values depend on the governing mechanism controlling behavior of coupling beams, flexure or shear, but criteria to determine this distinction is not specified in the document. For example, an element could be termed “flexurally governed” if flexural hinges form at the ends of the element prior to reaching its shear strength. For low amounts of longitudinal

reinforcement, flexural hinging could occur at moment values that are close to the expected yield moment (using anticipated material strength and neglecting strain hardening). Because of shear strength degradation at high displacements, the coupling beam might subsequently fail in shear although it could be initially classified as flexure dominated.

Table 1.1 – Modeling parameters for coupling beams in *ASCE/SEI 41-06* (see Fig. 1.3 for definition of parameters)

Reinforcement Configuration	$\frac{V}{b_w h\sqrt{f_c'}}$ [b]	Controlled by Flexure			Controlled by Shear		
		a	*b*	*c*	*d*	*e*	*c*
With conforming transverse reinforcement[a]	≤ 3	0.025	0.050	0.75	0.020	0.030	0.60
	≥ 6	0.020	0.040	0.50	0.016	0.024	0.30
With nonconforming transverse reinforcement[a]	≤ 3	0.020	0.035	0.50	0.012	0.025	0.40
	≥ 6	0.010	0.025	0.25	0.008	0.014	0.20
Diagonal reinforcement	n.a.	0.030	0.050	0.80	—	—	—

[a]Conforming transverse reinforcement consists of: (a) closed stirrups over entire beam length at a spacing ≤ *d/3*, and (b) strength of closed stirrups $V_s \geq 3/4$ of required shear strength of coupling beam; [b] f'_c in [lb/in^2]

Chord rotations of beams that are governed by shear are estimated using rotations *d* and *e* (see Table 1.1 and Fig. 1.3a). In contrast for beams governed by flexure, all post-yield chord rotation values (rotations *a* and *b*) are referenced to the chord rotation at yield. A shear force retention coefficient is given in Table 1.1 as parameter *c*, which is the fraction of shear at yielding retained at large displacements.

ASCE/SEI 41-06 defines the chord rotation at yield as:

$$\theta_y = \frac{M_y}{E_c I_{cr}} l_p \qquad (3)$$

where M_y represents the yield moment; E_c is the secant modulus of elasticity of concrete ($E_c = 57000\sqrt{f_c'}$ [psi]; $= 4730\sqrt{f_c'}$ [MPa]); I_{cr} represents the cracked moment of inertia of the cross section; and l_p is the plastic hinge length defined above. *ASCE/SEI 41-06* suggests estimating the cracked (effective) flexural and shear stiffness of coupling beams as 0.3 $E_c I_g$ and 0.4 $E_c A_{cv}$, respectively, where A_w is the gross cross sectional area resisting shear ($b_w h$). It should be noted that the shear stiffness value used in *ASCE/SEI 41-06* can be obtained by using the

relationship between E_c and shear modulus of concrete, $G_c=E_c/[2(1+\nu)]$, with ν (Poisson's ratio) taken equal to 0.25. This observation implies that any shear stiffness degradation due to concrete cracking is neglected. An evaluation of existing coupling beam tests found in the literature (Ihtiyar and Breña, 2006) revealed that shear stiffness in coupling beams can degrade substantially even at small deformation demands. Paulay (1971) had already highlighted the importance of considering shear distortions when computing stiffness in short coupling beams and the significant loss of stiffness experienced after cracking.

One of the limitations of estimating flexural stiffness only using a fraction of gross moment of inertia (e.g. 0.3 I_g) is that these reductions are insensitive to effects of span-to-depth ratio on cracked stiffness. Paulay and Priestley (1992) indicated that cracked moment of inertia of coupling beams varies depending on beam aspect ratio and recommended that I_{cr} for conventionally reinforced coupling beams be calculated using:

$$I_{cr} = \frac{0.2 I_g}{\left[1+3\left(\frac{h}{l_n}\right)^2\right]} \qquad (4)$$

Alternatively, *ASCE/SEI 41-06* allows use of experimental results to generate the backbone response of elements instead of using tabulated modelling parameters. These two approaches are schematically illustrated in Fig. 1.3, where part (a) of the figure shows the generic shape of backbone curves that is used in combination with values from Table 1.1 to construct the backbone curve for a particular element, and part (b) of the figure indicates a possible way of generating an experimentally derived backbone curve and a simplified curve that one might obtain with the tabular procedure in *ASCE/SEI 41-06* for this particular element.

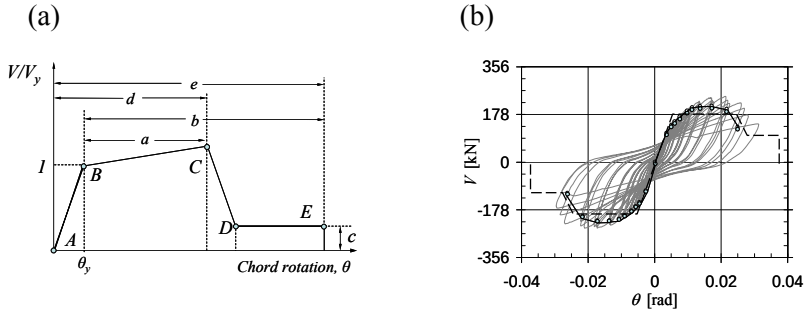

Figure 1.3 – Construction of backbone curves using (a) tabulated values (a), or (b) experimental results (Ihtiyar and Breña 2007)

1.2.3 Components of chord rotation in coupling beams

It has been mentioned that chord rotation is used as the primary deformation parameter to construct backbone envelopes in coupling beams. In short deep members deformation components other than those induced by flexure might play an important role in the total element deformation. In the case of coupling beams, shear forces and bar slippage introduce important components of deformation to the total chord rotation. These components are illustrated graphically in Fig. 1.4. In particular, the chord rotation obtained from flexural and shear deformations after cracking should be included if one hopes to capture the ascending branch in the shear force-chord rotation behavior of these components. Bar slippage (Fig. 1.4c), an important contributor to total deformation at large displacements, may not play an important role in post-cracking, pre-yield deformations and can therefore be neglected at small displacement demands.

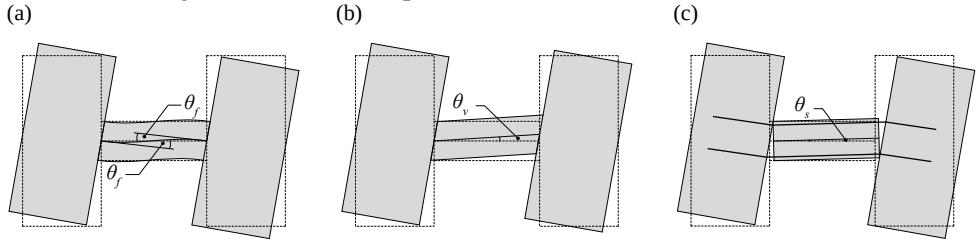

Figure 1.4 – Coupling beam components of chord rotation: (a) flexural deformation; (b) shear deformation; and (c) bar slippage

2. INFLUENCE OF REINFORCEMENT LAYOUT ON BEHAVIOR: EXPERIMENTAL RESPONSE AND COMPARISON WITH *ASCE/SEI 41-06* BACKBONE CURVES

Coupling beam specimens were tested at the University of Massachusetts Amherst with the primary intent to investigate effects of reinforcing characteristics on the observed failure mode and evaluate the quality of backbone curves constructed using procedures in *FEMA 356* (parent document of *ASCE/SEI 41-06*). Specimens were designed using a concrete mix with a nominal compressive strength of 30 MPa. Nominal yield strength of the longitudinal and transverse reinforcement was 410 MPa, except for specimen CB-2 that had transverse reinforcement consisting of deformed wire with a nominal yield strength of 580 MPA. Table 2.1 lists the main geometric and as-built material properties of all specimens. Figure 2.1 illustrates the geometry and reinforcement patterns of the four specimens tested in this research. As observed, the main parameters that were varied were beam span, transverse reinforcement content, and longitudinal reinforcement content. Full details of the specimens were presented by Ihtiyar and Breña (2007).

Loading was applied to the coupling beams by means of two stiff concrete walls constructed on each end of the specimens. Lateral loading was applied to the top of the walls using a stiff steel element that imposed equal lateral displacement to both walls (Fig. 2.2). Given the geometry of the test setup, an applied lateral force Q generated shear forces at the ends of the coupling beams equal to $Q\ h_{pin}/(l_b+l_w)$, giving shears of 1.1 and 0.8 times Q for the short (CB-1 and CB-3) and long (CB-2 and CB-4) specimens, respectively. Lateral force was applied cyclically in sets of three cycles at pre-defined amplitudes. Lateral loading was controlled by force in pre-yield stages and subsequently changed to displacement control at post-yield stages. At loading stages below the estimated yield shear force (V_y), the applied loading amplitudes were 1/3, 2/3, and 3/3 of V_y. The lateral displacement at the top of the walls at V_y was defined as the displacement at yield. Subsequent loading was applied in increments of 0.5 times the yield displacement. Loading was stopped as specimens began to lose strength at higher applied displacements since the primary intent was to evaluate the stiffness of the loading branch. Only specimen CB-4 was taken to much higher displacements because it was designed to be flexurally dominated and its shear retention capacity at large displacements was of particular interest.

Table 2.1 – Primary as-built parameters of coupling beam specimens

Specimen	d	l_n	Longitudinal steel			Transverse steel			f_c
			A_s	f_{yl}	ρ_l[(a)]	A_v	f_{yt}	ρ_v	
	[mm]	[mm]	[mm^2]	[MPa]	[%]	[mm^2]	[MPa]	[%]	[MPa]
CB-1	340	510	600	517	0.69	142	524	1.1	39
CB-2	340	1020	851	448	0.99	52	607	0.13	39
CB-3	270	510	860[(b)]	517	1.25	142	524	1.1	31
CB-4	340	1020	400	517	0.47	142	524	1.1	30

[(a)] $\rho_l = A_s/bd$; $\rho_v = A_v/b_w s$; [(b)] Includes lowermost layer of distributed longitudinal web reinforcement (2 No. 4 bars, Fig. 2.1a).

2.1 Measured hysteretic response

Specimen response was primarily evaluated by examining their shear force-chord rotation response. The measured shear force in the coupling beams was compared with calculated values obtained from backbone curves constructed according to *ASCE/SEI 41-06* and the failure mode observed during the tests. All calculated strengths (flexural or shear) were obtained using the measured material properties of each specimen and presence of additional web reinforcement, if any. Only specimen CB-2 had insufficient shear strength, according to Eq. 2, to reach yielding of the longitudinal reinforcement (Table 2.2). All other specimens were expected to be able to develop flexural yielding and attainement of flexural strength at the ends of the beams (compare V_{end} –measured shear at beam-wall connection– with V_n –calculated strength according to Eq. (2)– in Table 2.2).

Plastic hinging was not expected for any specimen except CB-4 (with low flexural reinforcement ratio and a relatively long span).

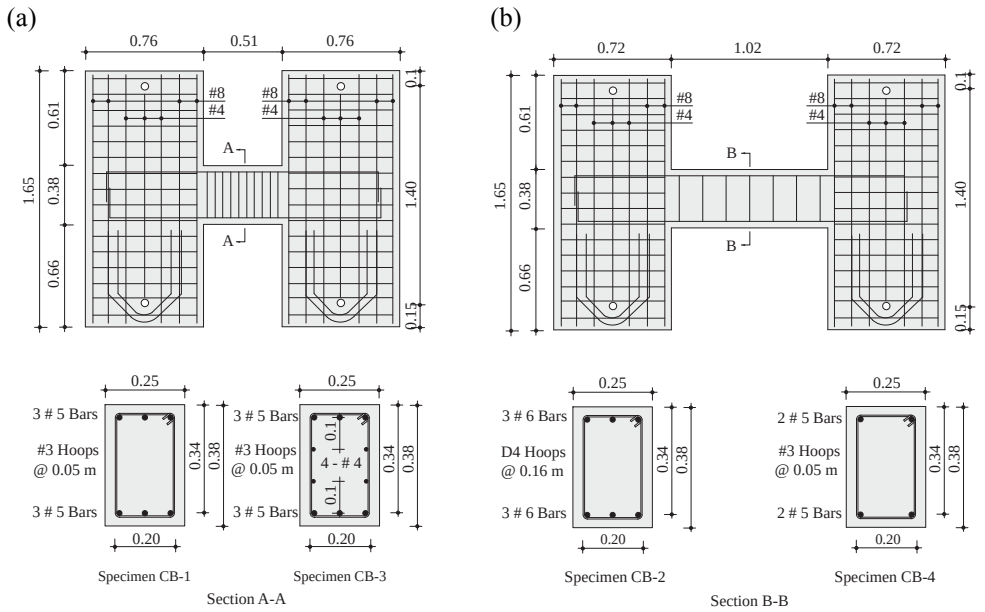

Figure 2.1 – Specimen geometry and reinforcing details (dimensions in [m]): (a) specimens CB-1 and CB-3; and (b) specimen CB-2 and CB-4

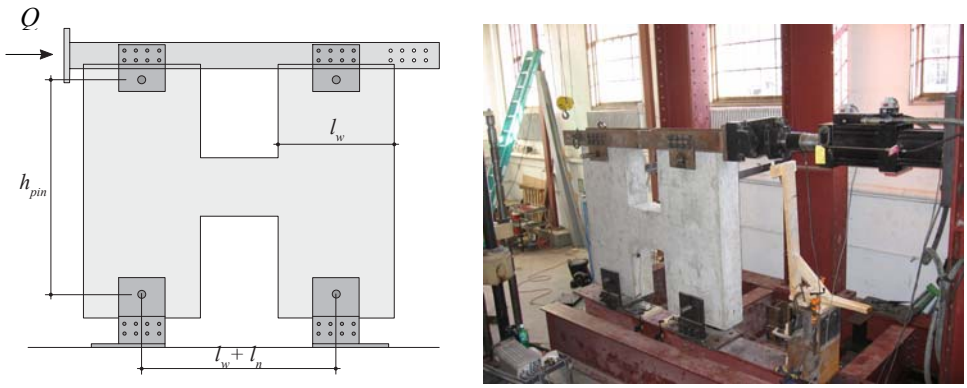

Figure 2.2 – Experimental setup: (a) general geometry and (b) specimen in test rig

Table 2.2 – Summary of measured shear force and chord rotation in beams

Specimen	$Q_{test,pk}$ [kN]	$V_{y,test}$ [a] [kN]	$V_{test,pk}$ [kN]	$\theta_{test,pk}$ [rad]	V_{end} [kN]	V_n [b] [kN]
CB-1	436	371	480	0.0311	492	709
CB-2	221	227	275	0.0076	319	187
CB-3	460	447	506	0.0299	575	693
CB-4	193	141	240	0.0214	168	647

[a] Determined using strain gauges adhered to flexural reinforcment
[b] Using Eq. (2)

The cyclic (hysteretic) shear force-chord rotation behavior of the four beams tested in the experimental program are shown in Fig. 2.3, from which several response features can be highlighted. Specimens CB-1 and CB-3 (short span) exhibited essentially similar hysteretic characteristics. Both specimens reached approximately the same shear force and were able to develop similar chord rotations at yield and peak shear force. The influence of horizontal web reinforcement in CB-3 did not affect the hysteretic response significantly.

The highly contrasting behavior of specimens CB-2 and CB-4, although with the same span-to-depth ratio, was primarily caused by the significantly different amounts of transverse reinforcement. Transverse reinforcement in CB-2 was barely sufficient to maintain shear strength after formation of the first diagonal crack and resulted in a brittle failure mode with no yielding of the longitudinal reinforcement. On the other hand, CB-4 had a very ductile response as a result of low flexural strength and relatively high shear capacity. Specimen CB-4 was the only beam that had a higher shear strength than required to develop plastic hinging and spread of plasticity near beam ends.

2.2 Comparison of backbone curves with experimental force-deformation curves

Backbone curves are useful for static nonlinear analyses conducted as part of performance-based design or assessment of structures. The tests conducted provided an opportunity to conduct an evaluation of the results of four beams with distinctly different behavior. Backbone curves for the four tested coupling beams were constructed using recommendations from *ASCE/SEI 41-06* (dashed lines in Fig. 2.3). Several modifications on the construction of these curves, however, were introduced on the basis of test results (Ihtiyar and Breña 2007):

(1) Shear deformations using gross elastic properties were included to calculate the chord rotation at yield. The calculated chord rotation at yield using Eq. (3), which neglects the component of deformation due to shear forces grossly underestimated the chord rotation measured experimentally.

(2) Although it could be argued that short coupling beams are governed by shear, all specimens except CB-2 were initially considered to be governed by flexure. It was assumed that if yielding was developed prior to reaching the shear strength then the beam would be governed by flexure.

(3) The shear force at yield (V_y) and the shear force at ultimate (V_{end}) were assumed acting at the end of the beams when yield penetration was insignificant (less than *d/4*). When plastic hinging developed (specimen CB-4) the shear force at ultimate was assumed acting at the end of the plastified region (V_{hinge}).

(4) To obtain a better stiffness correlation with the measured hysteresis curves (solid lines in Fig. 2.3), the cracked moment of inertia recommended by Paulay and Priestley (1992, Eq. 3) and a shear deformation component based on cracked section properties were used to estimate the chord rotation at yield. The cracked shear deformation component ($\theta_{v\text{-}cr}$) was estimated using measured distortions during the tests (Ihtiyar and Breña, 2007). This last modification resulted in better agreement with the experimental curves.

Shear force at yield and ultimate were calculated using measured material properties. Chord rotations were obtained using the coefficients listed in Table 1.1 for beams controlled by flexure (specimens CB-1, CB-3, CB-4) or those for beams controlled by shear (specimen CB-2). For comparison, the curve for flexurally controlled behavior was also constructed specimen CB-2 (Fig. 2.3c). A similar approach to construct backbone curves based on *FEMA 356*, including the background for these modifications, were discussed by Ihtiyar and Breña (2007).

Table 3.1 – Comparison of measured and calculated shear forces and chord rotations at peak load (values in parentheses obtained considering the four recommendations listed above)

Specimen	$V_{test,\,pk}$ [kN]	$\theta_{test,\,pk}$ [rad]	V_{calc}[(a)] [kN]	θ_{calc} [rad]	$\frac{V_{test,pk}}{V_{calc}}$	$\frac{\theta_{test,pk}}{\theta_{calc}}$
CB-1	480	0.0311	492	0.0219	0.98	1.42
			(492)	(0.0340)	(0.98)	(0.91)
CB-2	275	0.0076	187	0.0110	1.47	0.69
			(320)[(b)]	(0.0245)[(b)]	(0.86)	(0.43)
CB-3	506	0.0299	575	0.0223	0.88	1.34
			(575)	(0.0376)	(0.88)	(0.79)
CB-4	240	0.0214	205	0.0253	1.17	0.85
			(205)	(0.0296)	(1.17)	(0.72)
				Average	1.13	1.07
					(0.97)	(0.72)
				CoV	0.23	0.34
					(0.15)	(0.29)

[(a)]Shear at development of flexural strength of beam.
[(b)]Using curve corresponding to flexurally controlled beam.

(a) Specimen CB-1

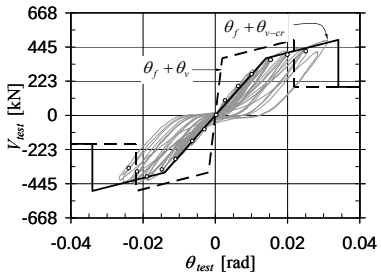

(b) Specimen CB-3

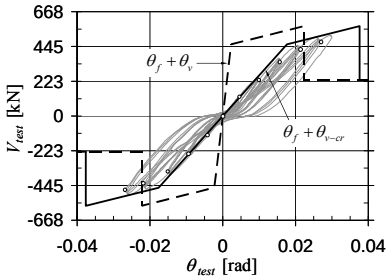

(c) Specimen CB-2

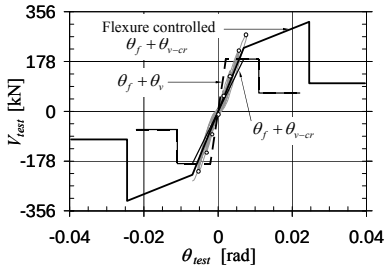

(d) Specimen CB-4

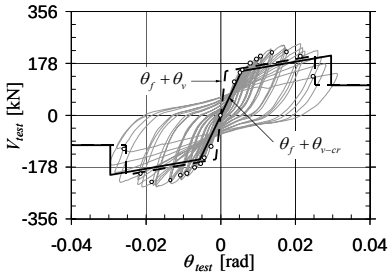

Figure 2.3 – Hysteretic response of coupling beam specimens and comparison with backbone curves (dashed lines correspond to *ASCE/SEI 41-06* and solid lines correspond to proposed modifications)

3. EVALUATION OF TEST RESULTS AND BACKBONE ENVELOPES USING STRESS FIELDS

3.1 Stress fields for modelling of reinforced concrete shear walls

Stress fields were developed from direct application of the lower bound theorem of the theory of plasticity to reinforced concrete members by Drucker (1961), Fig. 3.1c. Using a rigid-plastic assumption for material behaviour (Figs. 3.1a,b) a series of stress fields have been developed for use in design and assessement of structural concrete (Nielsen et al. 1978, Müller 1978, Marti 1980; Muttoni 1989, Muttoni et al. 1997).

These stress fields, termed rigid-plastic (discontinuous) stress fields, generally provide safe estimates of the failure load and allow the designer a clear understanding of the load-carrying mechanisms of a structure. This can for instance be seen in Figs. 3.2a,b where two licit stress fields for the same problem (a deep beam subjected to distributed loading) are shown. In the first one (Fig. 3.2a) load is carried by fan action, whereas in the second (Fig. 3.2b) load is carried by arching action. The corresponding truss models, showing further detail of their differences, are also shown (Figs. 3.2c,d).

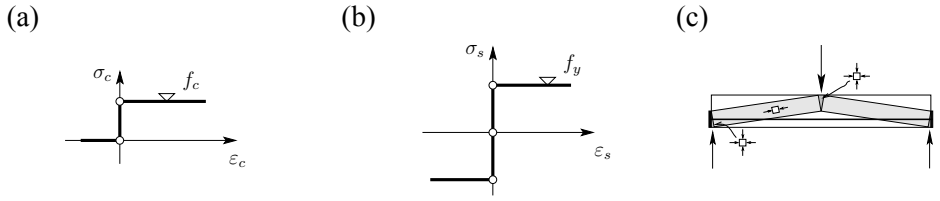

Figure 3.1 – Rigid-plastic stress fields: (a) rigid-plastic constitutive law for concrete (without tensile strength); (b) rigid-plastic constitutive law for steel; and (c) first rigid-plastic stress field for a beam subjected to concentrated loading proposed by Drucker (1961)

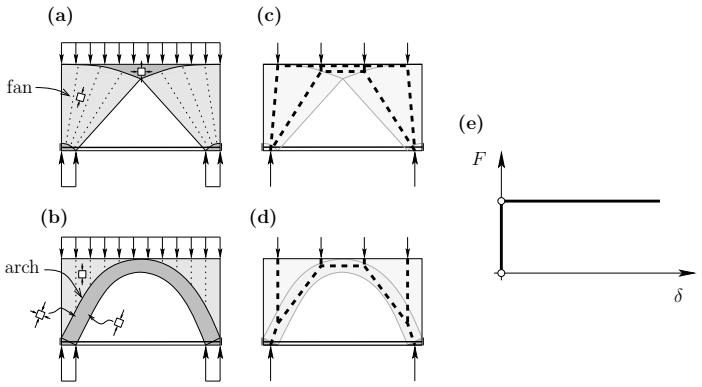

Figure 3.2 – Rigid-plastic stress fields for deep beam subjected to distributed loading: (a,b) fan-shaped and arch-shaped load-carrying mechanisms; (c,d) corresponding truss models; and (e) force-deflection curve

Application of rigid-plastic stress fields may, however, have two drawbacks. First, there is no unique solution to a given problem (refer to Fig. 3.2a,b), which requires a certain level of experience for choosing the most adequate load-carrying mechanism. Second, no information is provided on the deformation capacity of the members due to the assumption of rigid-plastic behaviour of materials (Fig. 3.2e). This consideration may limit their use for solution to certain classes of problems like seismic behaviour of coupling beams, where displacements and rotations are the basic input for structural analysis (refer to first section of this paper).

In order to overcome these two problems, elastic-plastic (continuous) stress fields have recently been developed (Fernández Ruiz and Muttoni, 2007). They account for the same hypotheses as rigid-plastic stress fields but considering an elastic-perfectly plastic behaviour for materials (Fig. 3.3). This allows calculating the strains in concrete as well as the displacements of the member. Since the longitudinal and transverse strains of compression struts are known, the influence of transverse cracking on the compressive strength of concrete can also be systematically considered. To that aim, a strength reduction factor affecting

concrete strength can be introduced using, for instance, the modified compression field theory relationship (Vecchio and Collins 1986):

$$f_{ce} = f_c \cdot \eta_\varepsilon \quad \text{where}: \eta_\varepsilon = \frac{1}{0.8 + 170\varepsilon_{tr}} \leq 1.0 \tag{5}$$

where ε_{tr} is the transverse strain perpendicular to applied stress in concrete.

An efficient implementation of such fields using the finite element method is described and discussed in Fernández Ruiz and Muttoni (2007).

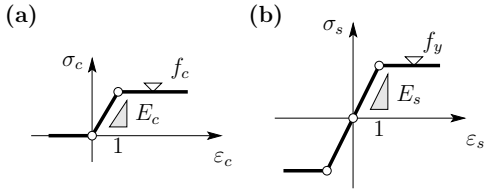

Figure 3.3 – Assumed material behaviour in elastic-plastic stress fields for: (a) concrete; and (b) reinforcing steel

The suitability of elastic-plastic (continuous) stress fields for describing the behaviour of shear walls and coupling beams with respect to monotonic loading has been investigated within this research with reference to the tests of Maier and Thürlimann (1985). The geometry of two specimens is shown in Fig. 3.4. The specimens analyzed, named S1 and S2, were subjected to varying levels of axial and shear forces.

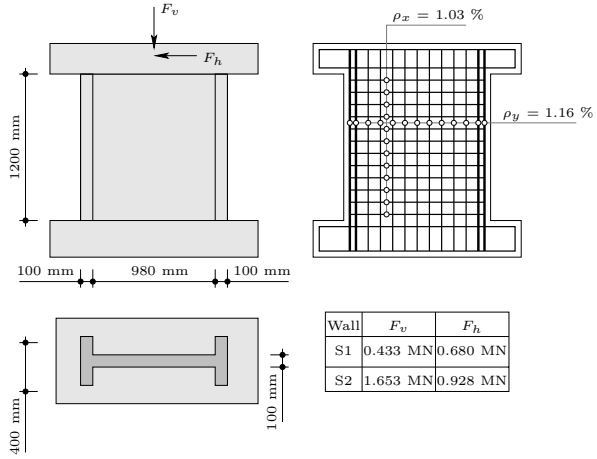

Wall	F_v	F_h
S1	0.433 MN	0.680 MN
S2	1.653 MN	0.928 MN

Figure 3.4 – Geometry and reinforcement layout of specimens S1 and S2 by Maier and Thürlimann (1985), f_c=36 MPa, E_c=34000 MPa, f_y=574 MPa, E_s=200000 MPa

The results obtained using elastic-plastic continuous stress fields are shown in Fig. 3.5. Excellent agreement is obtained with respect to the failure load (calculated failure loads equal to 1.01 and 0.98 of measured loads in specimens S1 and S2, respectively). Also, relatively good agremeent is obtained with respect to the deformation capacity of the members, with reasonable estimates of the deformation at reinforcement yielding or concrete crushing (Fig. 3.5 g). The corresponding rigid-plastic stress fields for the two specimens are also shown (Figs. 3.5 c,f), which facilitate viewing the actual force paths and provide a tool for design of vertical and horizontal reinforcement.

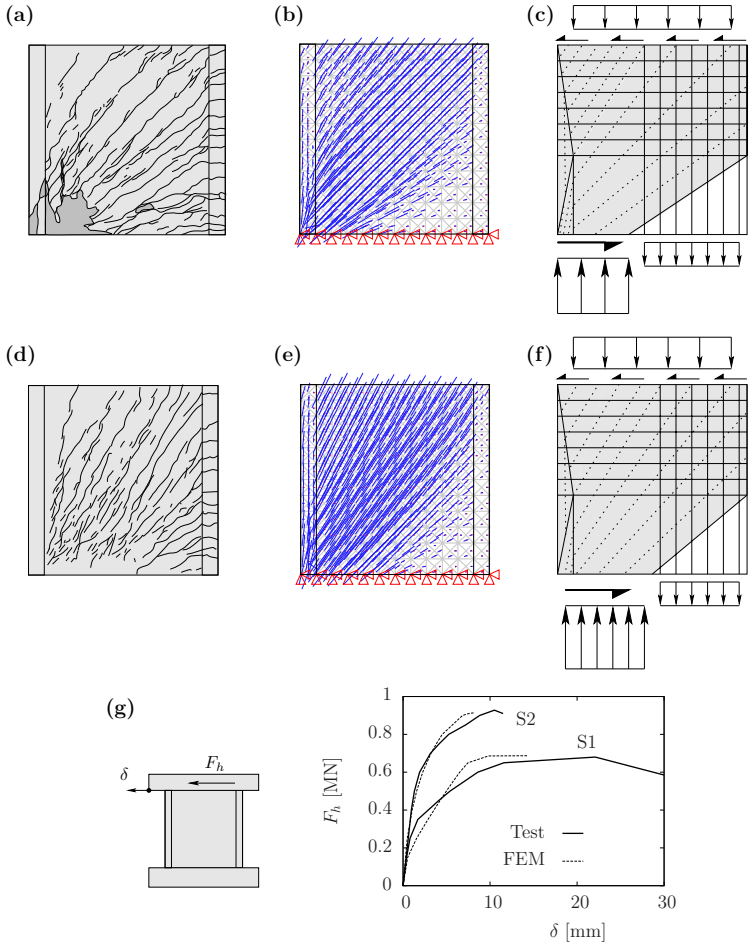

Figure 3.5 – Shear walls S1 and S2 (Maier and Thürlimann, 1985): (a) cracking pattern of S1 (after failure); (b) plot of elastic-plastic stress field concrete principal stress directions for S1; (c) rigid-plastic stress field for S1; (d) cracking pattern in S2 (at 95 % of failure load); (e) elastic-plastic stress field concrete principal stress directions for S2; (f) rigid-plastic stress field for S2; and (g) comparison of measured/computed horizontal deflection for both shear walls.

3.2 Comparison of elastic-plastic stress fields to test results on coupling beams subjected to reverse loading

Application of elastic-plastic stress fields is investigated in this section with reference to the tests presented previously in section 2.1. Figure 3.6 shows the calculated stress fields at peak load for the four coupling beam specimens. The stress fields are consistent with the observed cracking patterns during the tests and are therefore representative of the actual force path. Figure 3.7 shows the shear force – chord rotation results for the various specimens calculated using the material properties described in section 2. Also, in the same figure, the shear force – chord rotation response is plotted assuming a reduced modulus of concrete, equal to one-quarter of the actual one, to simulate the reduction in stiffness after cracking. A summary of main results for both analyses can be found in Table 3.1.

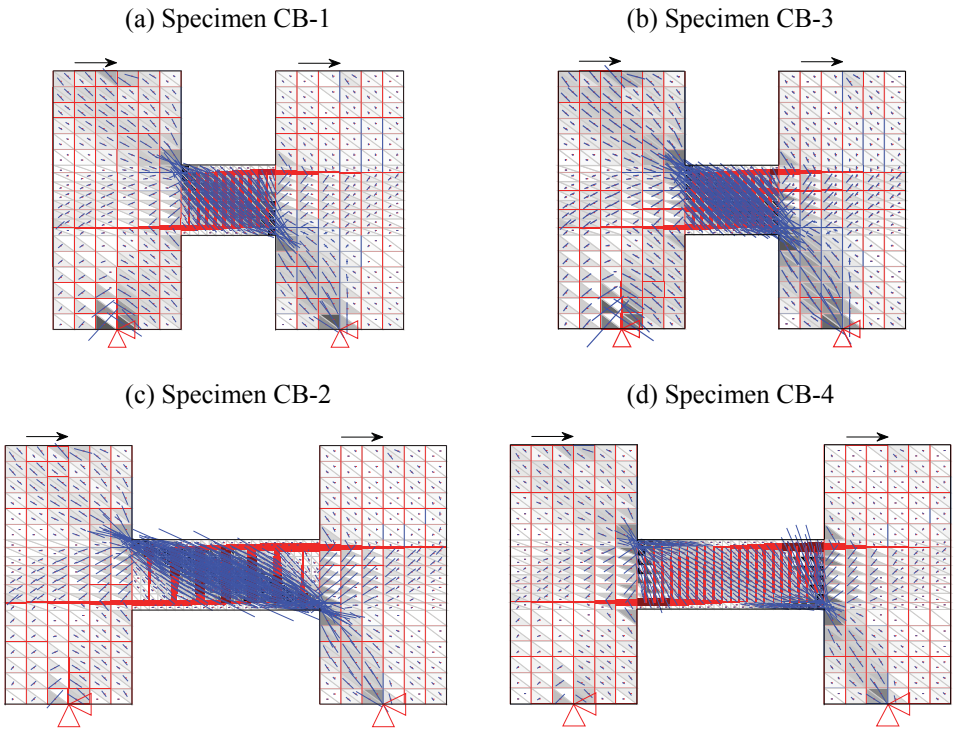

Figure 3.6 – Elastic-plastic stress fields calculated for coupling beam specimens

(a) Specimen CB-1

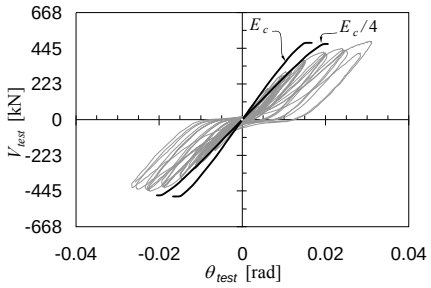

(b) Specimen CB-3

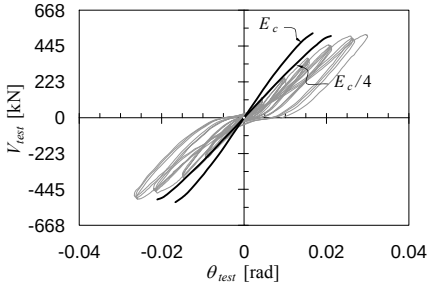

(c) Specimen CB-2

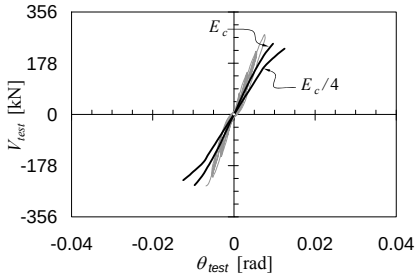

(d) Specimen CB-4

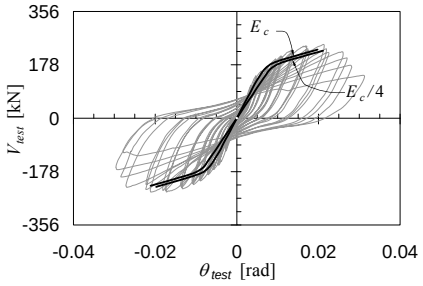

Figure 3.7 – Comparison of shear force – chord rotation results for elastic-plastic stress fields with measured data

The comparison between tests with stress field modelling yields to the following observations:

1. Failure loads are accurately predicted for all members, regardless of the slenderness, reinforcement layout and failure mode.
2. Failure loads are little sensitive to reductions in the modulus of elasticity of concrete. Nevertheless, small reductions in the failure load are obtained for softer modulus of elasticity as larger displacements develop (reducing concrete strength due to the factor η_ε)
3. The chord rotations are accurately estimated using the elastic (uncracked) modulus of elasticity of concrete for initial cycles of loading. Degradation in the modulus of elasticity due to cyclic loading plays a significant role in the deformational behaviour, as confirmed by a better match between calculated force-deformation envelopes and measured cyclic response in particular for shorter elements when reducing the modulus to $E_c/4$.

Stress field results compared to backbone envelopes based on *ASCE/SEI 41-06* show that: (1) a significantly better estimation of the maximum load is obtained with a much lower value of CoV, and (2) safer estimates of the chord rotation at maximum load are obtained with a similar scatter of results.

Table 3.1 – Comparison of measured and calculated failure loads and chord rotations at maximum load (values in parentheses obtained using an effective modulus of elasticity of concrete equal to $E_c/4$).

Specimen	$V_{test\text{-}pk}$ [kN]	$\theta_{test\text{-}pk}$ [rad]	V_{calc} [kN]	θ_{calc} [rad]	$\frac{V_{test}}{V_{calc}}$	$\frac{\theta_{test}}{\theta_{calc}}$
CB-1	480	0.0311	479	0.0167	1.00	1.86
			(472)	(0.0206)	(1.02)	(1.51)
CB-2	275	0.0076	246	0.0096	1.12	0.79
			(229)	(0.0125)	(1.20)	(0.61)
CB-3	506	0.0299	524	0.0166	0.97	1.80
			(508)	(0.0211)	(1.00)	(1.42)
CB-4	240	0.0214	228	0.0197	1.05	1.09
			(225)	(0.0211)	(1.07)	(1.01)
				Average	1.03	1.39
					(1.07)	(1.14)
				CoV	0.06	0.38
					(0.09)	(0.36)

The results show that stress field modelling is a promising technique that can capture the backbone behaviour of coupling beams. It allows a consistent approach that accounts for the various mechanical and geometric parameters with a very limited number of parameters and hypotheses (Fernández-Ruiz and Muttoni, 2007). The reduction in stiffness introduced for large displacements and relatively short deep coupling beams is consistent with what previous researchers have identified (e.g. Paulay, 1971a; Park and Ang, 1985; Ihtiyar and Breña, 2007).

4. FUTURE WORK

The authors are currently working on a formulation to compute stiffness degradation as a function of concrete loading history (number of cycles and maximum deformation demand). This work will allow automatic development of elastic-plastic stress fields for development of backbone envelope curves for use in performance-based seismic design or assessment, and improvement of chord rotation estimates.

5. CONCLUSIONS

This paper discusses various techniques to construct backbone curves for coupling beams subjected to seismic loading, and compares the techniques with a set of experiments conducted on large-scale components. Its main conclusions are:

1. Slenderness, reinforcement layout, amount of transverse reinforcement and failure mode (bending or shear) have a significant influence on the strength and behaviour (deformation capacity) of coupling beams.
2. The influence of these parameters, however, is not accurately considered in current performance-based methods for design of such members. This leads to significant scatter of backbone curve generation.
3. Backbone curves constructed using available seismic assessment documents (e.g. *ASCE/SEI 41-06*) can reasonably represent the envelope behavior of coupling beams if certain modifications are introduced to existing recommendations. In particular, it is important to include all relevant deformation components to reasonably capture the envelope behaviour.
4. Modelling the envelope response of coupling beams based on elastic-plastic stress fields provides a rational approach for estimating strength and deformation capacity at yield and peak load. This technique allows accounting for the influence of the various mechanical and geometric parameters (including the slenderness of the member and the amount and layout of flexural and shear reinforcement) on behavior.
5. Stiffness degradation of concrete subjected to cyclic loading with large amplitudes plays a significant role in the shear force – chord rotation relationship of coupling beams.

ACKNOWLEDGEMENTS

The authors would like to acknowledge Onur Ihtiyar who performed the experimental work described within this paper as part of his Masters thesis at the University of Massachusetts Amherst during 2007.

NOTATION

A_{cv} = concrete cross section resisting shear
A_s = area of longitudinal steel
A_v = area of transverse steel within spacing, s
E_c = modulus of elasticity of concrete
E_s = modulus of elasticity of steel
F = force
F_H = horizontal force
F_V = vertical force
G_c = shear modulus of concrete
I_{cr} = cracked moment of inertia
I_g = gross moment of inertia
M = bending moment
M_y = yield moment

Q = horizontal applied force
$Q_{test,\ pk}$ = maximum applied horizontal force
V = shear force
V_{calc} = maximum calculated shear force
V_{end} = shear computed at end of beam
V_{hinge} = shear computed at center of plastic hinge
V_n = nominal shear strength of beam
V_s = contribution of transverse steel to shear strength
V_{test} = shear force in coupling beam specimens
$V_{test,\ pk}$ = maximum measured shear force
V_y = shear force at yield of longitudinal reinforcement
$V_{y,\ test}$ = measured beam shear at yielding of longitudinal reinforcement
b_w = web width
d = flexural (effective) depth of beam
f_{ce} = effective concrete compressive strength
f_c = concrete cylindrical compressive strength
f'_c = 28-day concrete compressive strength
f_y = steel stress at yield
f_{yl} = longitudinal steel stress at yield
f_{yt} = transverse steel stress at yield
h = depth of beam
h_{pin} = height between loading and support pins in specimens
l_n = coupling beam length
l_p = plastic hinge length
l_w = wall length
s = spacing of transverse reinforcement
α_c = aspect ratio factor (for use in Eq. 2)
δ = displacement
ν = Poisson's ratio
θ = coupling beam chord rotation
θ_{calc} = calculated chord rotation at maximum load
θ_f = flexural component of chord rotation
θ_v = shear component of chord rotation
$\theta_{v\text{-}cr}$ = shear component of chord rotation using cracked properties
θ_s = bar slip component of chord rotation
$\theta_{test,\ pk}$ = measured chord rotation at maximum load
θ_y = chord rotation at yield
ε_c = axial strain in concrete
ε_s = strain in a reinforcing bar
ε_{tr} = transverse strain in concrete
η_ε = strength reduction factor accounting for transverse cracking
ρ_l = longitudinal reinforcement ratio

ρ_v = transverse reinforcement ratio
σ_c = stress in concrete
σ_s = stress in a steel bar

REFERENCES

American Concrete Institute (ACI) (2008). "Building Code Requirements for Structural Concrete (318-08) and Commentary (318R-08).", *ACI 318-08*, Detroit, MI.

American Society of Civil Engineers (2000). "Prestandard and Commentary for the Seismic Rehabilitation of Buildings", *FEMA Publication 356*, Washington, D.C.

Applied Technology Council (ATC-43 project) (1999a). "Evaluation of Earthquake Damaged Concrete and Masonry Wall Buildings –Basic Procedures Manual", *FEMA Publication 306*, Washington, D.C.

Barney, G.B., Shiu, K.N., Rabbat, B.G., Fiorato, A.E., Russell, H.G., and Corley, W.G. (1980). "Behavior of Coupling Beams under Load Reversals". *Research and Development Bulletin RD068.01B*. Portland Cement Association, 22 p.

Beck H. (1962). "Contribution to Analysis of Coupled Shear Walls." *ACI Journal*. Vol. 59, No. 8, pp. 1055-1070.

Canbolat, B.A., Parra-Montesinos, G.J., and Wight, J.K. (2005). "Experimental Study on Seismic Behavior of High-Performance Fiber-Reinforced Cement Composite Coupling Beams." *ACI Structural Journal*, Vol. 102, No. 1, pp. 159-166.

Coull A., and Choudhury J.R. (1967). "Analysis of Coupled Shear Walls." *ACI Journal*, Vol. 64, No. 9, pp. 587-593.

Coull A., and Puri R.D. (1968). "Analysis of Coupled Shear Walls of Variable Cross-Section." *Building Science*, Vol. 2, No. 4, pp. 313-320.

Coull A., Puri R.D., and Tottenham H. (1973). "Numerical Elastic Analysis of Coupled Shear Walls." *Proceedings of the Institution of Civil Engineers. Part 1 – Design & Construction*, Vol. 55, pp. 109-128.

Drucker, D. C. (1961). "On Structural Concrete and the Theorems of Limit Analysis." *Publications, International Association for Bridge and Structural Engineering*. Vol. 21, pp. 49-59

Elkholy, I.A.S., and Robinson, H. (1974). "Inelastic Analysis of Coupled Shear Walls." *Building Science*, Vol. 9, No. 1, pp. 1-8.

Fernández-Ruiz, M., and Muttoni, A. (2007). "On Development of Suitable Stress Fields for Structural Concrete." *ACI Structural Journal*. Vol. 104, No. 4, pp.

495-502.

Galano, L. and Vignoli, A. (2000). "Seismic Behavior of Short Coupling Beams with Different Reinforcement Layouts." *ACI Structural Journal*. Vol .97, No. 6, pp. 876-885

Glueck, J. (1973). "Elasto-Plastic Analysis of Coupled Shear Walls." *Journal of the Structural Division, ASCE*, Vol. 99 (ST8), pp. 1743-1760.

Harries, K.A., Mitchell, D., Redwood, R.D., and Cook, W.D. (1997). "Seismic Design of Coupled Walls – A Case for Mixed Construction." *Canadian Journal of Civil Engineering*. Vol. 24, No. 3, pp. 448-459.

Ihtiyar, O. and Breña, S.F. (2006). "Force-Deformation Response of Conventionally Reinforced Coupling Beams: Evaluation of FEMA 356 and FEMA 306." *2006 8th U.S. National Conference on Earthquake Engineering*. Paper no. 701. San Francisco, CA.

Ihtiyar, O. and Breña, S.F. (2007). "Assessment of FEMA 356 Techniques for Orthogonally Reinforced Coupling Beams through Experimental Testing." *2007 ASCE Structures Congress: Structural Engineering Research Frontiers*. Long Beach, CA.

International Conference of Building Officials (1997). 1997 "Uniform Building Code" Volume 2, Whittier, CA.

International Code Council (2009). 2009 "International Building Code", Whittier, CA.

Mahin, S.A. and Bertero, V.V. (1976). "Nonlinear Seismic Response of a Coupled Wall System." *Journal of the Structural Division, Proceedings ASCE*. Vol. 102, No. ST9, pp. 1759-1780

Maier, J., and Thürlimann, B. (1985) "Tests on shear walls" (in German: "Bruchversuche an Stahlbetonscheiben"), Institut *für Baustatik und Konstruktion ETH Zürich*, Bericht Nr. 8003-1, 1985

Marti, P. (1980), "On the plastic analysis of reinforced concrete" (in German, "Zur plastischen Berechnung von Stahlbeton"), *Institut für Baustatik und Konstruction, Bericht Nr. 104*, ETH Zürich, 1980, 175 pp.

Muttoni, A. (1989), "The applicability of the theory of plasticity in the design of reinforced concrete" (in German, "Die Andwendbarkeit der Plastizitätstheorie in der Bemessung von Stahlbeton"), *Institut für Baustatik und Konstruktion, ETH Zürich*, Bericht Nr. 176, 1989, 159 pp.

Muttoni, A., Schwartz, J. and Thürlimann, B. (1997), "Design of concrete structures with stress fields", *Birkhaüser / Springer*, 1997, 145 pp.

Müller, P. (1978) "Plastic calculus of reinforced concrete disks and beams" (in

German, “Plastische Berechnung von Stahlbetonscheiben und –balken”), *Institut für Baustatik und Konstruction, ETH Zürich*, Bericht Nr. 83, 1978, 160 pp.

Nielsen, M. P., Braestrup, M. W., Jensen, B. C. and Bach, F. (1978), “Concrete plasticity, beam shear –shear in joints– punching shear”, *Danish Society for Structural Science and Engineering*, Special Publication, 1978, 129 pp.

Park, Y-J, and Ang, A.H-S. (1985). “Mechanistic seismic damage model for reinforced concrete.” *Journal of Structural Engineering*, Vol. 111, No. 4, pp. 722-739.

Paulay, T. (1970). “Elasto-Plastic Analysis of Coupled Shear Walls.” *Journal of the American Concrete Institute*. Vol. 67, No. 11, pp. 915-922.

Paulay, T. (1971a). “Coupling Beams of Reinforced Concrete Shear Walls.” *Journal of the Structural Division, Proceedings ASCE*. Vol. 97, No. ST3, pp. 843-861.

Paulay, T. (1971b). “Simulated Seismic Loading of Spandrel Beams.” *Journal of the Structural Division, Proceedings ASCE*. Vol. 97, No. ST9, pp. 2407-2419.

Paulay, T., and Binney, J.R., (1974). “Diagonally Reinforced Coupling Beams of Shear Walls.” *Shear in Reinforced Concrete, ACI Publication SP-42*, pp. 579-598

Paulay, T. and Santhakumar, A.R. (1976). “Ductile Behavior of Coupled Shear Walls.” *Journal of the Structural Division, Proceedings ASCE*, Vol. 102, No. ST1, pp. 99-108.

Takayanagi, T. and Schnobrich, W.C. (1979). “Non-linear Analysis of Coupled Wall Systems.” *Earthquake Engineering & Structural Dynamics*., Vol. 7, No. 1, pp. 1-22.

Tassios, T.P., Moretti, M., and Bezas A. (1996). “On the Behavior and Ductility of Reinforced Concrete Coupling Beams of Shear Walls.” *ACI Structural Journal,* Vol. 93, No. 6, pp. 711-720.

Vecchio, F. J. and Collins, M. P. (1986) “The modified compression field theory for reinforced concrete elements subjected to shear”, *ACI Journal*, Vol. 83, No. 2, March-April, 1986, pp. 219-231.